ChemPubSoc Europe

DOI: 10.1002/cssc.201500493

CHEMSUSCHEM Full Papers

Unravelling the Ru-Catalyzed Hydrogenolysis of Biomass-Based Polyols under Neutral and Acidic Conditions

Peter J. C. Hausoul, Leila Negahdar, Kai Schute, and Regina Palkovits*[a]

The aqueous Ru/C-catalyzed hydrogenolysis of biomass-based polyols such as erythritol, xylitol, sorbitol, and cellobitol is studied under neutral and acidic conditions. For the first time, the complete product spectrum of C_2–C_6 polyols is identified and, based on a thorough analysis of the reaction mixtures, a comprehensive reaction mechanism is proposed, which consists of (de)hydrogenation, epimerization, decarbonylation, and deoxygenation reactions. The data reveal that the Ru-catalyzed deoxygenation reaction is highly selective for the cleavage of terminal hydroxyl groups. Changing from neutral to acidic conditions suppresses decarbonylation, consequently increasing the selectivity towards deoxygenation.

Introduction

Cellulosic biomass is an abundant renewable resource, which holds great promise for the sustainable production of fuels and chemicals.[1–6] By employing selective depolymerization methods, several defined platform chemicals can be obtained from cellulose (Scheme 1). For example, acid-catalyzed hydrolysis yields glucose, which serves as precursor for platform molecules such as HMF and levulinic acid.[7,8] Alternatively, when acid-catalyzed hydrolysis is combined with metal-catalyzed hydrogenation, sorbitol or hexitols are obtained directly as the main products.[9–11] Particularly Ru-based catalysts exhibit high selectivities towards hexitols under relatively mild conditions. Excellent hexitol yields are obtained for cellulose, which has been converted to cello-oligomers by acidic ball milling.[12–17] At elevated temperatures, hydrogenolytic C–C and C–O bond breaking reactions increase and short-chain polyols such as propylene and ethylene glycol are formed.[18–21] In addition, it has been shown that the product spectrum can also be steered towards light alkanes and hexane.[22,23] This clearly demonstrates the high versatility of Ru-catalyzed hydrolytic hydrogenation and hydrogenolysis of cellulose. Yet improving the selectivity towards target products remains a major challenge. Hence, it is imperative to gain a better understanding of the role of the metal catalyst as well as the acid co-catalyst to enable a rational catalyst design. Thus far, a limited number of studies have provided insight into the reaction mechanism by studying the resulting product mixture. Drawing on earlier work concerning Cu, Montassier attributed the product mixture obtained by the aqueous Ru-catalyzed hydrogenolysis of polyols to the occurrence of (de)hydrogenation, dehydroxylation, retro-aldolization, and retro-Michael reactions.[24,25] Clear evidence in support of the retro-aldol condensation reaction was provided by Furney et al., who studied the Cu- and Ni-catalyzed hydrogenolysis of 1,3-diol model compounds in the presence of 1 M NaOH.[26] Recently, Shanks et al. studied the product mixtures of nine different polyols in the presence of Ru/C and CaO.[27] In addition to the retro-aldol reaction, decarbonylation was proposed to account for the observed product mixture. This suggests that two fundamentally different C–C cleavage reactions may occur under hydrogenolysis conditions. It should, however, be noted that these studies were conducted under basic conditions. To the best of our knowledge, the effect of acid on the product spectrum of the hydrogenolysis of higher polyols has not been studied in detail. Here, we present the results of the Ru/C-catalyzed hydrogenolysis of biomass-based polyols under neutral and acidic conditions. The product spectrum and reaction network under neutral conditions is studied using erythritol, xylitol, and sorbitol. Subsequently, the influence of the addition of catalytic amounts of silicotungstic acid ($H_4[W_{12}SiO_{40}]$) on the product spectrum is studied using sorbitol and cellobiitol (as model compound for cello-oligomers). Based on these results and H/D exchange experiments, a comprehensive mechanism is proposed for the Ru/C-catalyzed hydrogenolysis reaction under acidic conditions.

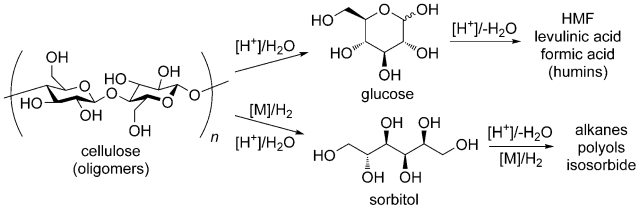

Scheme 1. Hydrolysis and hydrolytic hydrogenation of cellulose.

[a] *Dr. P. J. C. Hausoul, Dr. L. Negahdar, K. Schute, Prof. Dr. R. Palkovits*
Institut für Technische und Makromolekulare Chemie
RWTH Aachen University
Worringerweg 2, 52074 Aachen (Germany)
E-mail: palkovits@itmc.rwth-aachen.de

Supporting Information for this article is available on the WWW under http://dx.doi.org/10.1002/cssc.201500493.

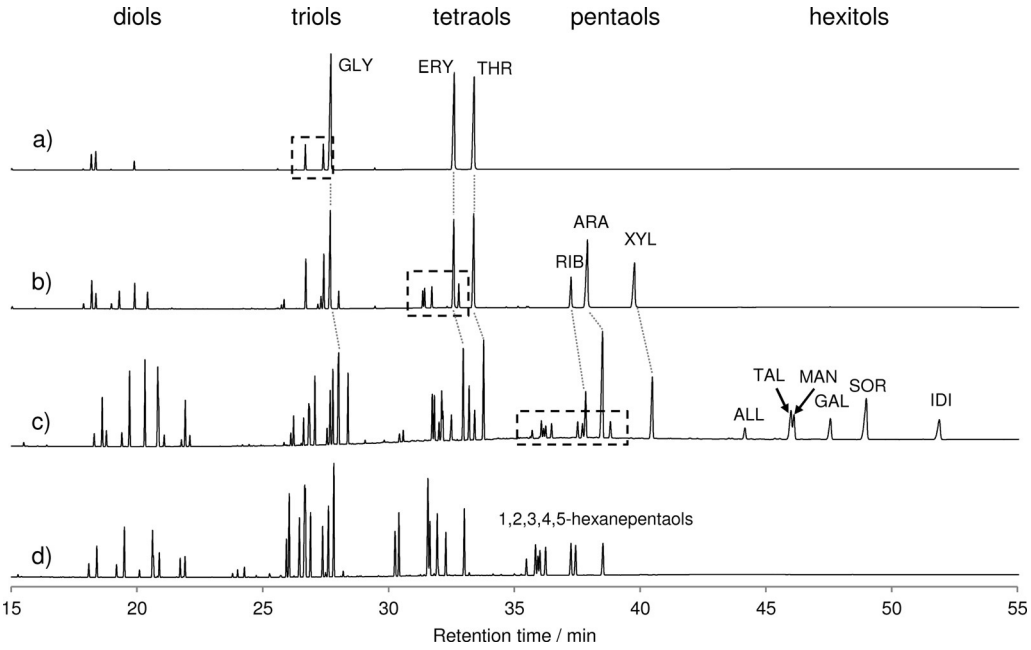

Figure 1. GC chromatograms (DB-23 column) of the peracetylated product mixtures of ERY (a), XYL (b), SOR (c), and RAM (d); 1-deoxygenated products are boxed. Conditions: 2.0 g substrate, 400 mg Ru/C (5 wt%), 20 mL H_2O, 3 h, 6 MPa H_2, 423 K.

Results and Discussion

Product spectrum under neutral conditions

Ru/C-catalyzed hydrogenolysis of erythritol (ERY), xylitol (XYL), and sorbitol (SOR) was performed in water at 423 K under 6 MPa H_2. Samples were taken periodically and peracetylated prior to analysis by GC(–MS) and LC–MS. Figure 1 shows the mixtures obtained after 3 h of reaction. In all cases the starting polyol is accompanied by all of its possible stereoisomers [i.e., for ERY: threitol (THR); for XYL: ribitol (RIB) and arabitol (ARA); and for the SOR: allitol (ALL), talitol (TAL), mannitol (MAN), galactitol (GAL), and iditol (IDI)]. The identity of these isomers was confirmed by comparison with authentic samples. As shown, the chromatogram can be divided into five regions containing diols, triols, tetraols, pentaols, and hexitols. In the pentaols region of the SOR reaction (Figure 1c), RIB, ARA, and XYL are observed, providing evidence for C–C cleavage reactions. In the same region, a set of eight hexanepentaols (boxed) is observed. The structure of these compounds was determined using the 6-deoxy sugar L-rhamnose (RAM, Scheme 2) After a mild hydrogenation (16 h, 423 K) eight isomers of 1,2,3,4,5-hexanepentaols are obtained, which correspond exactly to those observed in the product spectrum of SOR. This mixture was further reacted for 3 h at 423 K, yielding the chromatogram shown in Figure 1d. Interestingly, pentitols, tetritols, glycerol (GLY), and ethyleneglycol (EG) are not observed in the product spectrum of RAM. Apparently, a reductive C–O cleavage or deoxygenation reaction occurs selectively at the terminal hydroxyl groups. Analogously, in the reaction of XYL (Figure 1b), a set of four isomers of 1,2,3,4-pentanetetraols (boxed) is observed next to ERY and THR. In the reaction of ERY (Figure 1a), two isomers of 1,2,3-butanetriol (boxed) are observed next to GLY. It is also noteworthy that all compounds observed in the mixture of ERY are also observed in that of XYL. The same holds for the product mixtures of XYL and SOR. Thus, any additional peaks in a particular region can be attributed to compounds with an extended carbon chain. Based on this and HPLC–electrospray ionization (ESI)–MS data, all major groups of compounds could be identified. These data confirm that Ru/C catalyzes stereoisomerization and C–C and C–O bond-cleavage reactions. Below, these reactions pathways are examined in more detail.

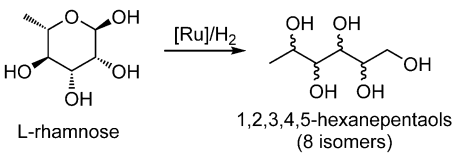

Scheme 2. Ru/C-catalyzed hydrogenation of RAM.

Stereoisomerization

The formation of stereoisomers of SOR such as MAN and GAL is commonly observed in reductive transformations of cellulose and glucose. As the stereochemistry is of little relevance for bulk chemical applications, reaction yields are typically expressed as summed hexitols. However, as discussed by Shanks et al.,[27] the formation stereoisomers can yield valuable insight into the reaction mechanism. Stereoisomerization likely occurs through metal-catalyzed epimerization. To gain more insight into the reaction mechanism, H/D exchange was studied for SOR and α-methylglucoside (AMG). AMG was selected as a model for the cyclic units of cello-oligomers. Catalytic H/D

exchange is well known and provides a simple means for the perdeuteration of carbohydrates.[28–31] The exchange mechanism is considered to involve adsorbed alkoxide species that are reversibly dehydrogenated to $\eta^2(C,O)$-bonded carbonyls. Surprisingly, only little is known of the relative reactivities of the different positions of sugar alcohols and carbohydrates.[32] Reactions were performed at 373 K in D_2O under 6 MPa H_2 using Ru/C and studied by quantitative ^{13}C NMR spectroscopy (see the Supporting Information). Apart from slightly upfield-shifted signals due to α- (−0.05 ppm) and β-deuteration (−0.005 ppm), no additional signals appeared. This confirms that under these conditions the exchange proceeds with retention of the stereochemistry. In all cases, an initial induction period of 0.5 h was observed, which is most likely due to the reduction of a thin oxide layer on the catalyst. After that, the non-deuterated signals decay in a first-order fashion. The extrapolated rate constants are shown in Scheme 3. In line with

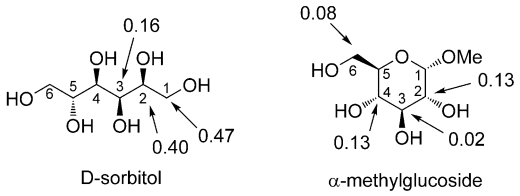

Scheme 3. Numbering scheme and rate constants (h^{-1}) of H/D exchange of SOR and AMG. Conditions: 2.0 g substrate, 0.4 g Ru/C (5 wt%), 20 mL D_2O, 6 MPa H_2, 373 K.

literature reports, H/D exchange only occurred on hydroxylated positions. The rate constants show that aldose formation (0.47 h^{-1}) is preferred over 2-ketose formation (0.40 h^{-1}). The rate constant for 3-ketose formation (0.16 h^{-1}) is significantly smaller and suggests that for the innermost positions steric hindrance or strong adsorption may play a role. Compared to SOR, the rate constants of AMG are all smaller (0.02–0.13 h^{-1}), confirming that the ring structure complicates dehydrogenation. This indicates that the cyclic units of hydrogenated cello-oligomers are less prone to react at the catalyst surface than the terminal SOR moiety. Above 373 K, SOR is mostly converted to other hexitols. Figure 2 shows the evolution of the relative composition of hexitol isomers at 423 K. Initially, SOR is rapidly converted to MAN and IDI. Over time ALL, GAL and TAL are also formed in significant quantities and the composition changes towards equilibrium. The more rapid formation of MAN and IDI demonstrates that the 2- and 5-positions are considerably more reactive than the 3- and 4-positions (Scheme 4).

The results are in line with the H/D exchange data discussed above. Similar observations have also been reported for the epimerization of hexitols catalyzed by Ni/kieselgur.[33] Epimerization is proposed to proceed via the conversion of the $\eta^2(C,O)$-bonded carbonyl to a prochiral $\eta^1(O)$-mode. This species can either dissociate from the metal or revert back to $\eta^2(C,O)$-bonding with interconversion of the enantiotopic face. As H/D exchange occurs readily without racemization at lower temperatures, it can be inferred that the dissociation of

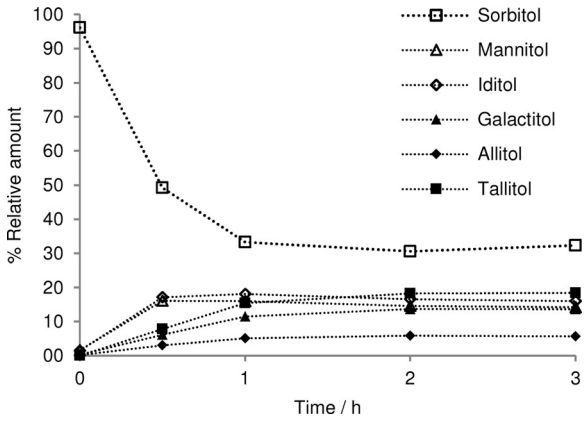

Figure 2. Hexitols composition. Conditions: 2.0 g substrate, 400 mg Ru/C (5 wt%), 20 mL H_2O, 6 MPa H_2, 423 K).

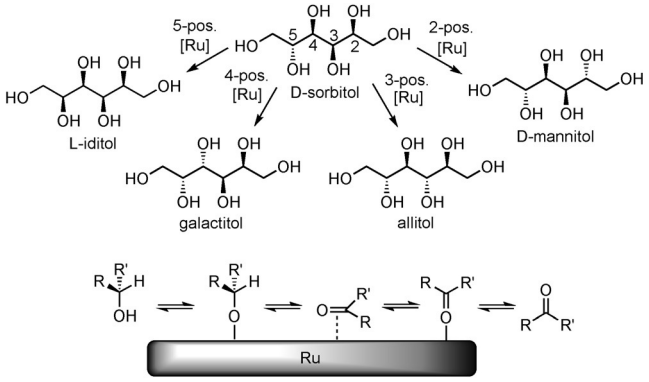

Scheme 4. Epimerization of SOR and proposed epimerization mechanism on Ru/C.

$\eta^2(C,O)$-bonded carbonyl is the rate-determining step of epimerization.

C–C bond cleavage

As discussed above, the occurrence of C–C bond-breaking reactions is well known in the field of metal-catalyzed hydrogenolysis. Particularly retro-aldol condensation and decarbonylation are often cited to account for the formation of short-chain compounds.[25–27] Both reactions are considered to involve an initial dehydrogenation step to yield aldose or ketose intermediates before cleavage.

The retro-aldol reaction can, in principle, cleave all C–C bonds of the polyol depending on the site of dehydrogenation (i.e., leading to C_1/C_5, C_2/C_4, and C_3/C_3 fragments) whereas decarbonylation selectively cleaves terminal C–C bonds. Accordingly, different reaction profiles are to be expected for these mechanisms. For example, the methanol synthesis catalyst $CuO/ZnO/Al_2O_3$ shows high selectivity for short-chain polyols such as EG, 1,2-PrD, and GLY at low conversions.[34] Figure 3a shows the evolution of hexitols, hexanepentaols, pentitols, tetritols, and GLY in the reaction of SOR at 423 K (other products are not shown for clarity). Clearly, pentitols are the main prod-

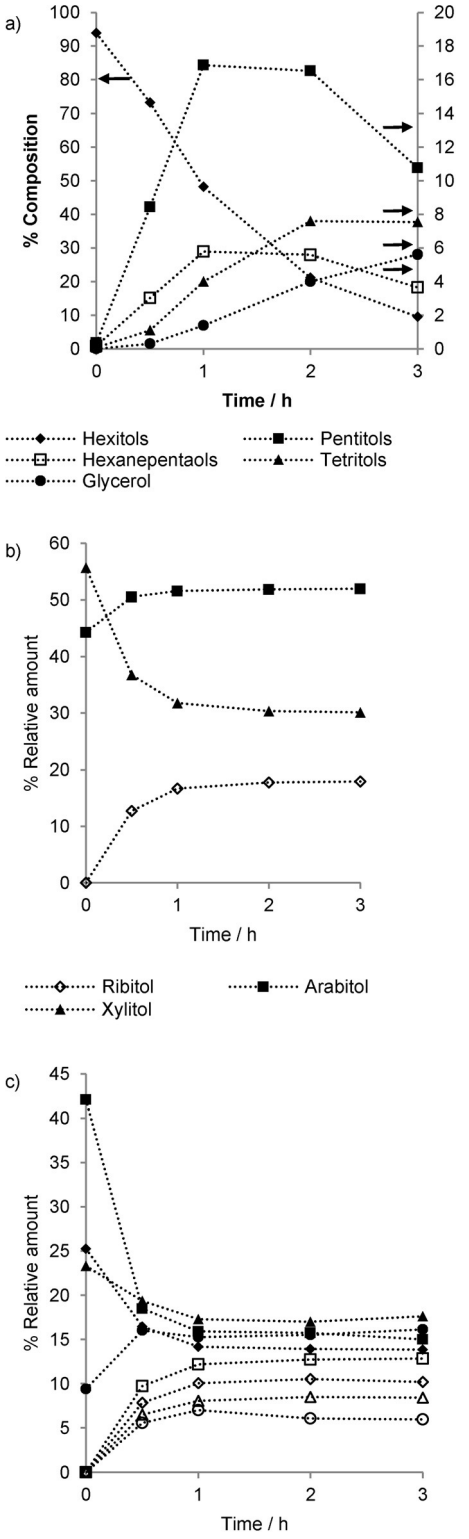

Figure 3. Ru/C-catalyzed hydrogenolysis of SOR (a), pentitols composition (b), and hexanepentaols composition (c). Conditions: 2.0 g substrate, 400 mg Ru/C (5 wt%), 20 mL H_2O, 6 MPa H_2, 423 K.

uct of the reaction, suggesting a decarbonylation reaction. After exhibiting a maximum at 1 h, the amount decreases and the amounts of tetritols and GLY increase. The relative composition of pentitols (Figure 3b) evidences that initially ARA and

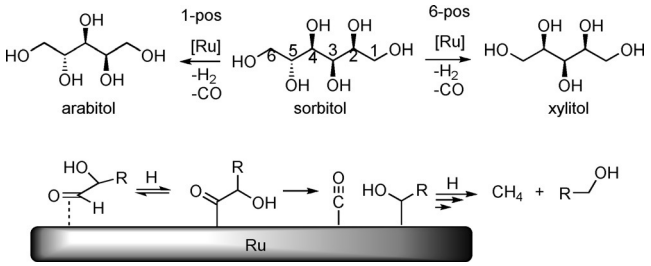

Scheme 5. Decarbonylation of SOR and proposed reaction mechanism on Ru/C.

XYL are formed in roughly equal amounts. ARA and XYL can be obtained from SOR by decarbonylation at the 1- and 6-positions, respectively (Scheme 5). Various studies confirmed that the heterogeneous decarbonylation mechanism involves an initial dehydrogenation reaction to yield an adsorbed aldehyde.[35] Activation of the aldehydic H atom, in turn, leads to a surface-bound acyl species, which can undergo C–C cleavage to yield adsorbed CO and an alkyl species.

Addition of hydrogen atoms to these species results in the formation of the corresponding alcohols and methane. This was confirmed by GC analysis of the gas phase, which showed the presence of only H_2 and CH_4. The data presented herein clearly identify decarbonylation as the primary C–C bond-breaking reaction under neutral conditions. Of course, this does not exclude the possibility of a retro-aldol reaction occurring at higher temperatures or in the presence of basic co-catalysts. Further studies are required to study the differences in product distribution arising from the participation of the retro-aldol reaction.

C–O bond cleavage

The results obtained for RAM (Figure 1d) confirm that the first deoxygenation step occurs selectively at the terminal positions of the polyol chain. This is rather counterintuitive as dehydration reactions generally proceed via the acid-catalyzed E_1 mechanism, which would favor the internal positions. This, however, is not observed. Possible mechanisms accounting for the observed dehydroxylation include a direct metal-catalyzed C–O activation or a dehydration reaction.

An important hint regarding the deoxygenation mechanism is provided by the relative composition of hexanepentaols (Figure 3c). Initially, four of the eight possible isomers are formed from SOR. As time progresses, the other four isomers are also formed and the composition equilibrates. This suggests that the deoxygenation mechanism results in the racemization of one stereocenter (i.e., either the 2- or the 5-position, Scheme 6). This excludes a direct C–O activation and suggests the intermediacy of a sp^2 hybridization at the 2- and 5-positions, thus supporting a dehydration reaction. The dehydration of terminal hydroxyl groups is proposed to proceed via a concerted E_2 mechanism involving Lewis acid and basic sites (Scheme 5). First, a terminal hydroxyl group is adsorbed onto the catalyst. A metal hydroxyl species can then abstract

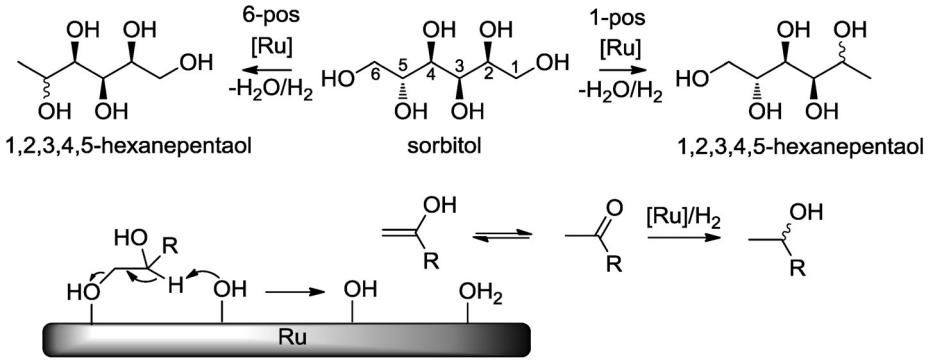

Scheme 6. Deoxygenation of SOR and proposed reaction mechanism on Ru/C.

a proton on the 2-position, leading to elimination of the primary hydroxyl group and formation of the enol. As such, the metal hydroxyl is regenerated. The enol, in turn, converts to the keto state and is ultimately hydrogenated to the alcohol. Numerous studies on the hydrogenolysis of GLY have repeatedly shown that 1,2-PrD is the main deoxygenation product irrespective of the metal catalyst used.[36] This raises the question whether the reaction is metal catalyzed or acid catalyzed. Reactions without Ru/C were performed at 433 K in the absence and presence of catalytic amounts of silicotungstic acid (STA). In the absence of STA, SOR remained completely stable for 3 h, whereas in the presence of STA 10% 1,4-sorbitan was formed as the sole product.[37] This indicates that under acidic conditions nucleophilic cyclodehydration is the preferred pathway. The absence of other products excludes possible rearrangement reactions (e.g., pinacol-type rearrangement)[38] and further confirms the role of the metal catalyst.

Reaction network

Based on the results discussed above, we propose that the product spectrum observed for SOR is the result of a reaction network of decarbonylation and deoxygenation steps as outlined in Scheme 7. The observation that the product spectra of XYL, ERY, and RAM are all included in the product spectrum of SOR (Figure 1) is well in line with the proposed reaction network. The substitution patterns after the first deoxygenation step could be assigned based on the high preference for terminal hydroxyl groups. Comparison of the diols section of the GC chromatograms of ERY, XYL, SOR, and RAM provides some important clues regarding the course of subsequent deoxygenation steps. In the chromatogram of ERY (Figure 4a), EG, 1,2-PrD, 2,3-butanediol (2,3-BuD), and 1,2-butanediol (1,2-BuD) are observed. 1,2-BuD can be obtained from the deoxygenation of 1,2,3-butanetriol at the 3-position whereas 2,3-BuD can be obtained from the deoxygenation at the 1-position. This confirms again that deoxygenation occurs on the outermost hydroxyl groups of the polyol chain independent of whether they are attached to a primary or a secondary carbon atom. Analogously, in the chromatogram of XYL (Figure 4b), three additional peaks are observed, which are assigned to 2,3-pentanediol (2,3-PeD) and 1,2-pentanediol (1,2-PeD). In the chromatogram of SOR (Figure 4c), another four peaks are observed, which are assigned to 2,3- and 3,4-hexanediol (2,3-/3,4-HeD). The same signals are also observed in the chromatogram of RAM (Figure 4d), with the exception that EG is absent. Scheme 8 shows the proposed course of the multiple deoxygenation steps of polyols. After the initial cleavage of a primary

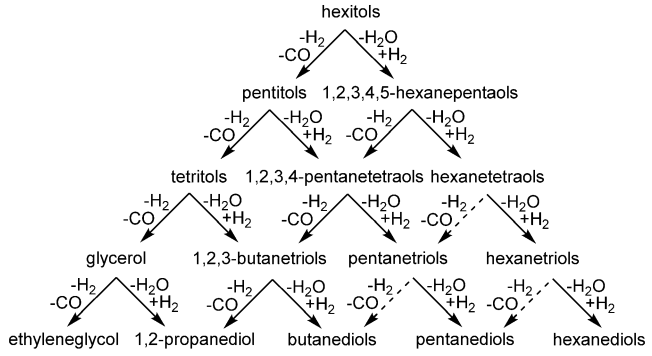

Scheme 7. Reaction network of the Ru/C-catalyzed hydrogenolysis of hexitols.

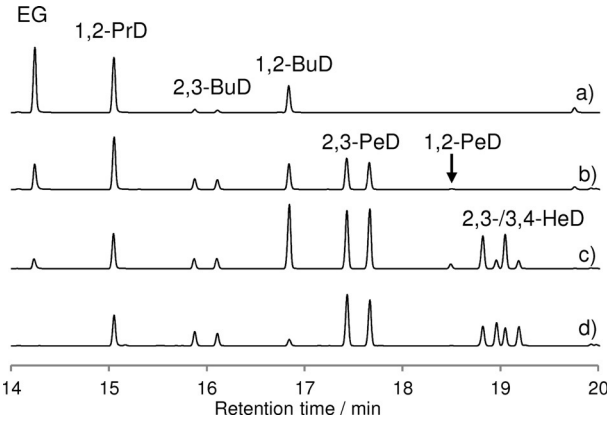

Figure 4. GC chromatograms (CP-SIL PONA CB column) of ERY (a), XYL (b), SOR (c), and RAM (d) reactions. Conditions: see Figure 1.

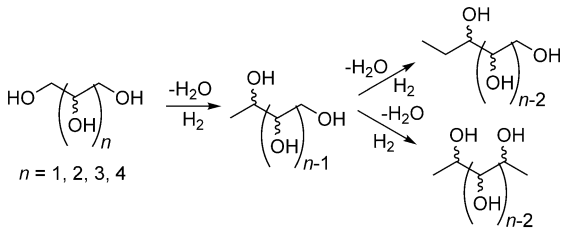

Scheme 8. Proposed deoxygenation of polyols.

hydroxyl group, a polyol with both terminal primary and terminal secondary hydroxyl groups is obtained. The results clearly show that these positions exhibit comparable reactivities. However, due to the simultaneous occurrence of decarbonylation and deoxygenation reactions, it is at present not possible to determine the selectivity difference between these positions. Kinetic analysis of the reaction network is currently performed to assess the rate constants and activation energies of the individual steps of the reaction mechanism.

Product spectrum under acidic conditions

The influence of acid on the hydrogenolysis reaction was studied by the addition of a catalytic amount of STA (0.24 mmol H^+) to the reactions of SOR and cellobiitol (CEL). Interestingly, the product spectrum of the reaction of SOR with acid is identical to that without (i.e., the same compounds are observed). Dehydration products such as sorbitan or isosorbide were not observed. Nevertheless, the evolution of the reaction mixture shows considerable differences. In the presence of STA, only 54% hexitol conversion is observed after 3 h (Figure 5a). This is significantly less than for the reaction without STA (Figure 3a), which amounted to 91%. The maximum amount of pentitols observed in the reaction decreased from 17% without to 7% with STA. Thus, the addition of acid inhibits decarbonylation. In contrast, the maximum amount of hexanepentaols increased from 6% without to 18% with acid. This demonstrates that the acidic co-catalyst has a strong influence on the selectivity of the hydrogenolysis reaction. This is particularly advantageous for the synthesis of liquid alkanes[23] as the degradation towards light alkanes and hydrogen consumption are decreased.

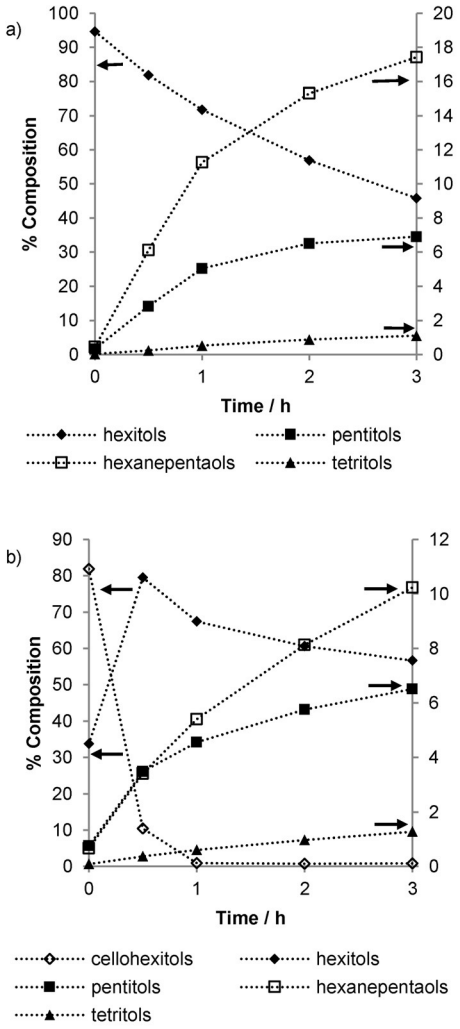

Figure 5. Ru/C-catalyzed hydrogenolysis of SOR (a) and CEL (b) with STA. Conditions: 2.0 g substrate, 400 mg Ru/C (5 wt%), 0.06 mmol STA, 20 mL H_2O, 6 MPa H_2,423 K; cellohexitol conversion was determined by performing LC–ESI–MS).

Cellohexitols

A kinetic study by Fukuoka et al. demonstrated that the slow depolymerization of cellulose and the simultaneous degradation by Ru severely limits hexitol yields to 40%.[39] The use of ball milling as pretreatment leads to significantly improved hexitol yields due to the formation of smaller (water-soluble) cello-oligomers.[12–17,39] Previous studies by us already showed that the hydrolytic hydrogenation of cello-oligomers such as cellobiose and cellotriose proceeds smoothly in the presence of Ru/C and STA.[40,41] Maximum hexitols yields of up to 80% are typically observed. Kinetic analysis of the reaction network revealed that the hydrogenation of cello-oligomers is considerably faster than hydrolysis, leading to 'cellohexitols' (i.e., cello-oligmers with a terminal hexitol unit). To access the hydrogenolysis of these oligomers we used cellobiose as model substrate (Scheme 9). Cellohexitols have been prepared by performing a mild hydrogenation of cellobiose at 373 K for 16 h. Figure 5b shows the conversion of the resulting cellohexitol mixture in the presence of STA at 423 K. The substrate is rapidly converted within 1 h, and a maximum yield of 79% hexitols is observed after 0.5 h. After that, the yield decreases and the amount of degradation products such as pentitols and hexanepentaols steadily increases. LC–ESI–MS data also confirm a direct degradation of the cello-

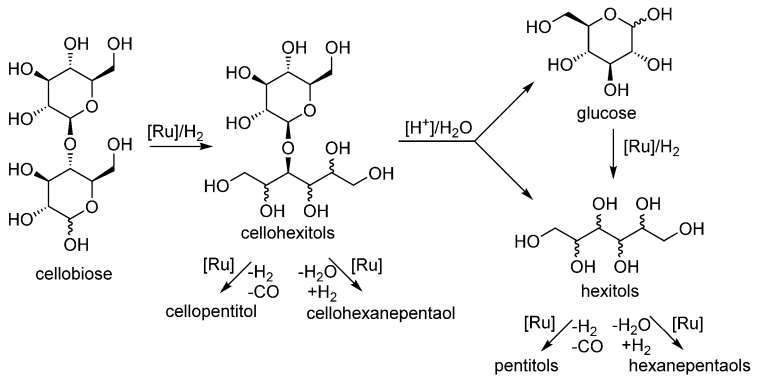

Scheme 9. Hydrolytic hydrogenation and hydrogenolysis of cellohexitols.

hexitols (see the Supporting Information). In contrast to the degradation network of SOR, degradation is much less extensive. This suggests that either the ether linkage or the high hydrolysis rate prevent further degradation.

Conclusions

The complete product spectra of C_2–C_6 polyols obtained through the hydrogenolysis of erythritol, xylitol, sorbitol, and cellobiitol have been identified. Analysis of the product spectrum revealed a complex reaction network consisting of stereoisomerization and C–C and C–O bond cleavage reactions. Based on H/D exchange data and the evolution of stereoisomers it is proposed that Ru/C catalyzes (de)hydrogenation, epimerization, decarbonylation, and dehydration reactions. The occurrence of retro-aldol condensation under the employed conditions could not be confirmed. As such, the primary Ru-catalyzed degradation pathways of higher polyols have been identified. The addition of silicotungstic acid lead to a suppression of decarbonylation and an enhancement of deoxygenation reactions. ESI–MS analysis of the reaction of cello-oligomers revealed that they are also degraded by Ru/C. With the insights gained and the methods developed for this study, it is now possible to close the mass balances of the liquid-phase products. It is expected that these results are also relevant for other catalyst systems and can benefit research aimed at the hydrogenolysis and/or hydrodeoxygenation of cellulosic biomass.

Experimental Section

D-(+)-cellobiose (>98%) and D-isosorbide (>98%) were obtained from Alfa Aesar. Ethylene glycol, 1,2-propanediol, glycerol, 1,2-butanediol, 2,3-butanediol, Ru/C (5 wt%), silicotungstic acid hydrate, allitol, D-talitol, L-iditol, and L-rhamnose monohydrate (>99%) were obtained from Sigma–Aldrich. D-(−)-Sorbitol (molecular Biology grade) was obtained from AppliChem. Galactitol, D-(+)-arabitol, mannitol, D-ribitol, xylitol, and erythritol were obtained from Supelco. Methyl-α-D-glucopyranoside (>99%) was obtained from Fluka. Deuteriumoxide (99.9% D) was obtained from Deutero GmbH. 1,4-sorbitan was prepared according to a literature procedure.[42]

Autoclave reactions

H/D exchange and hydrogenolysis experiments were performed in a 50 mL batch-type high-pressure autoclave reactor. Typically, substrate (2.0 g), Ru/C (0.4 g), and, where applicable, silicotungstic acid (0.175 g) were added into a glass-lined stainless steel reactor equipped with a sampling valve and charged with H_2O or D_2O (20 mL). The reactor was flushed by pressurizing and depressurizing three times with 6 MPa H_2 at room temperature. The reactor was pressurized with 6 MPa H_2 and then heated to the defined temperature (373–423 K). The time zero was set at the beginning of the isothermal reaction stage. For cellobiose and L-rhamnose, the reactions were performed in two stages. First, the reaction mixture was heated to 373 K for 16 h under 6 MPa H_2. After cooling the autoclave to room temperature, the gas phase was flushed twice and pressurized with 6 MPa H_2. Subsequently, the autoclave was heated to the desired reaction temperature. Progress of the reaction was monitored by periodically taking sample from the autoclave. Samples were filtered through a 25 μm polyamide filter prior to analysis.

NMR and GC–LC analysis

Sample solutions of H/D exchange reactions were measured directly by quantitative $^{13}C\{^1H\}$ NMR spectroscopy (Bruker Avance III 600 MHz, integrals were normalized to carbon atom; assignments were based on literature reference data).[42–44] In all other cases, 0.5 mL aliquots were dried using a Eppendorf Speedvac system (303 K, 8 h). The resulting residue was dissolved in 1 mL acetic anhydride/pyridine mixture (1:1 *v/v*) and left to react for 3 days at room temperature with periodic mixing and shaking. Subsequently, the sample solutions were measured by GC [Thermo Scientific Trace GC system equipped with an Agilent DB-23 column (internal diameter: 0.25 mm; length: 60 m; film thickness: 0.25 μm; isobaric: 0.1 MPa He; temperature gradient: 353–527 K) or a CP-SIL PONA CB column (internal diameter: 0.21 mm; length: 50 m; film thickness: 0.21 μm; isobaric: 0.1 MPa He; temperature gradient: 323–503 K)], GC–MS (Thermo Scientific Trace 1310 system equipped with a single quadrupole MS, EI+, 70 eV), and/or HPLC–ESI–MS [Shimadzu LC-MS 2020 system using a LiChrospher 100 column (RP-18e; length: 25 cm; particle size: 5 μm; binary gradient 30–50% B with the remainder being A (10 mM ammonium acetate aqueous solution with 0.1% formic acid); B: acetonitrile with 0.1% formic acid)]. All compounds were calibrated using the external standard method. Isomeric products were treated as possessing equal response factors. Hexitols were calibrated using sorbitol. The pentitols were calibrated using xylitol. The tetritols were calibrated using erythritol. The hydrogenated solutions of L-rhamnose and cellobiose were used to quantify hexanepentaols and cellohexitols, respectively.

Acknowledgements

The authors kindly thank Heike Fickers-Boltz, Elke Biener, and Hannelore Eschemann for the GC analyses; Noah Avraham for HPLC analyses; and Ines Bachmann for NMR analyses. This work was supported by the Robert Bosch Foundation within the Robert Bosch Junior Professorship for the efficient utilization of renewable resources. This work was performed as part of the Cluster of Excellence "Tailor-Made Fuels from Biomass" funded by the Excellence Initiative by the German federal and state governments to promote science and research at German universities.

Keywords: biomass · deoxygenation · hydrogenolysis · polyols · ruthenium

[1] C. H. Zhou, X. Xia, C. X. Lin, D. S. Tong, J. Beltramini, *Chem. Soc. Rev.* **2011**, *40*, 5588–5617.
[2] D. M. Alonso, S. G. Wettstein, J. A. Dumesic, *Chem. Soc. Rev.* **2012**, *41*, 8075–8098.
[3] J. P. Ma, W. Q. Yu, M. Wang, X. Q. Jia, F. Lu, J. Xu, *Chin. J. Catal.* **2013**, *34*, 492–507.
[4] Q. H. Zhang, F. Jerome, *ChemSusChem* **2013**, *6*, 2042–2044.
[5] M. Besson, P. Gallezot, C. Pinel, *Chem. Rev.* **2014**, *114*, 1827–1870.
[6] M. J. Climent, A. Corma, S. Iborra, *Green Chem.* **2014**, *16*, 516–547.
[7] R.-J. van Putten, J. C. van der Waal, E. de Jong, C. B. Rasrendra, C. B. Heeres, J. G. de Vries, *Chem. Rev.* **2013**, *113*, 1499–1597.
[8] F. Schüth, R. Rinaldi, N. Meine, M. Käldström, J. Hilgert, M. D. Kaufman Rechulski, *Catal. Today* **2014**, *234*, 24–30.

[9] X. R. Liu, X. C. Wang, S. X. Yao, Y. J. Jiang, J. Guan, X. D. Mu, *RSC Adv.* **2014**, *4*, 49501 – 49520.
[10] A. Ruppert, K. Weinberg, R. Palkovits, *Angew. Chem. Int. Ed.* **2012**, *51*, 2564 – 2601; *Angew. Chem.* **2012**, *124*, 2614 – 2654.
[11] C. Luo, S. Wang, H. Liu, *Angew. Chem. Int. Ed.* **2007**, *46*, 7636 – 7639; *Angew. Chem.* **2007**, *119*, 7780 – 7783.
[12] J. Geboers, S. van de Vyver, K. Carpentier, K. de Blochouse, P. Jacobs, B. Sels, *Chem. Commun.* **2010**, *46*, 3577 – 3579.
[13] J. Geboers, S. Van de Vyver, K. Carpentier, P. Jacobs, B. Sels, *Green Chem.* **2011**, *13*, 2167 – 2174.
[14] J. Geboers, S. Van de Vyver, K. Carpentier, P. Jacobs, B. Sels, *Chem. Commun.* **2011**, *47*, 5590 – 5592.
[15] J. Hilgert, N. Meine, R. Rinaldi, F. Schuth, *Energy Environ. Sci.* **2013**, *6*, 92 – 96.
[16] W. W. Zhu, H. M. Yang, J. Z. Chen, C. Chen, L. Guo, H. M. Gan, X. G. Zhao, Z. S. Hou, *Green Chem.* **2014**, *16*, 1534 – 1542.
[17] Y. Liu, L. G. Chen, T. J. Wang, Y. Xu, Q. Zhang, L. L. Ma, Y. H. Liao, N. Shi, *RSC Adv.* **2014**, *4*, 52402 – 52409.
[18] R. Palkovits, K. Tajvidi, J. Procelewska, R. Rinaldi, A. Ruppert, *Green Chem.* **2010**, *12*, 972 – 978.
[19] R. Palkovits, K. Tajvidi, A. M. Ruppert, J. Procelewska, *Chem. Commun.* **2011**, *47*, 576 – 578.
[20] Y. Liu, C. Luo, H. C. Liu, *Angew. Chem. Int. Ed.* **2012**, *51*, 3249 – 3253; *Angew. Chem.* **2012**, *124*, 3303 – 3307.
[21] A. Q. Wang, T. Zhang, *Acc. Chem. Res.* **2013**, *46*, 1377 – 1386.
[22] Y. Osaka, Y. Ikeda, D. Hashizume, M. Iwamoto, *Biomass Bioenergy* **2013**, *56*, 1 – 7.
[23] Y. Liu, L. Chen, T. Wang, Q. Zhang, C. Wang, J. Yan, L. Ma, *ACS Sustainable Chem. Eng.* **2015**, *3*, 1745 – 1755.
[24] D. K. Sohounloue, C. Montassier, J. Barbier, *React. Kinet. Catal. Lett.* **1983**, *22*, 391 – 397.
[25] C. Montassier, J. C. Menezo, L. C. Hoang, C. Renaud, J. Barbier, *J. Mol. Catal.* **1991**, *70*, 99 – 110.
[26] K. Wang, M. C. Hawley, T. D. Furney, *Ind. Eng. Chem. Res.* **1995**, *34*, 3766 – 3770.
[27] K. L. Deutsch, D. G. Lahr, B. H. Shanks, *Green Chem.* **2012**, *14*, 1635 – 1642.
[28] H. J. Koch, R. S. Stuart, *Carbohydr. Res.* **1977**, *59*, C1 – C6.
[29] H. J. Koch, R. S. Stuart, *Carbohydr. Res.* **1978**, *64*, 127 – 134.
[30] T. Maegawa, Y. Fujiwara, Y. Inagaki, Y. Mongushi, H. Sajiki, *Adv. Synth. Catal.* **2008**, *350*, 2215 – 2218.
[31] Y. Fujiwara, H. Iwata, Y. Sawama, Y. Monguchi, H. Sajiki, *Chem. Commun.* **2010**, *46*, 4977 – 4979.
[32] Y. Sawama, Y. Yabe, H. Iwata, Y. Fujiwara, Y. Monguchi, H. Sajiki, *Chem. Eur. J.* **2012**, *18*, 16436 – 16442.
[33] L. Wright, L. Hartmann, *J. Org. Chem.* **1961**, *26*, 1588 – 1596.
[34] K. Tajvidi, P. J. C. Hausoul, R. Palkovits, *ChemSusChem* **2014**, *7*, 1311 – 1317.
[35] M. Mavrikakis, M. A. Barteau, *J. Mol. Catal. A* **1998**, *131*, 135 – 147.
[36] J. ten Dam, U. Hanefeld, *ChemSusChem* **2011**, *4*, 1017 – 1034.
[37] J. U. Oltmanns, S. Palkovits, R. Palkovits, *Appl. Catal. A* **2013**, *456*, 168 – 173.
[38] W. B. Smith, *Tetrahedron* **2002**, *58*, 2091 – 2094.
[39] T. Komanoya, H. Kobayashi, K. Hara, W.-J. Chun, A. Fukuoka, *ChemCatChem* **2014**, *6*, 230 – 236.
[40] L. Negahdar, J. U. Oltmanns, S. Palkovits, R. Palkovits, *Appl. Catal. B* **2014**, *147*, 677 – 683.
[41] L. Negahdar, P. J. C. Hausoul, S. Palkovits, R. Palkovits, *Appl. Catal. B* **2015**, *166 – 167*, 460 – 464.
[42] G. J. Stockburger, US4297290A, **1981**.
[43] S. J. Angyal, R. Le Fur, *Carbohydr. Res.* **1980**, *84*, 201 – 209.
[44] S.-C. Ho, H. J. Koch, R. S. Stuart, *Carbohydr. Res.* **1978**, *64*, 251 – 256.

Received: April 8, 2015
Published online on September 3, 2015